Available online at www.sciencedirect.com

SciVerse ScienceDirect

Ceramics International 39 (2013) 8035–8042

CERAMICS INTERNATIONAL

www.elsevier.com/locate/ceramint

Effect of key operational factors on decolorization of methyl orange by multi-walled carbon nanotubes (MWCNTs)/TiO_2/CdS composite under simulated solar light irradiation

Ke Ouyang, Shan Xie*, Xiao'ou Ma

Department of Chemical and Environment Engineering, Wuyi University, Jiangmen 529020, Guangdong Province, China

Received 6 March 2013; accepted 20 March 2013
Available online 29 March 2013

Abstract

To improve the photocatalytic performance of TiO_2, a novel composite of TiO_2/CdS nanoparticles supported on multi-walled carbon nanotubes (MWCNTs) was prepared by a sol–gel method. This photocatalyst exhibited a strong photocatalytic activity for the decomposition of methyl orange (MO) in aqueous solution under simulated solar irradiation. The effects of key operational parameters, such as the initial MO concentration, initial pH values, catalyst dosage and the amount of additional H_2O_2, were systematically studied. The presence of all the anions examined (Cl^-, NO_3^-, SO_4^{2-}, CO_3^{2-} and PO_4^{3-}) had an inhibitory effect on the decolorization of MO. The photocatalyst had good stability, as when it was used for the fifth time, the decolorization efficiency was still about 98.7% after 80 min of irradiation. The simultaneous application of simulated solar and ultrasound irradiation resulted in increased decolorization compared to that achieved by photocatalysis alone. Possible decomposition mechanisms are discussed. The enhanced photocatalytic performance might be attributable to the matched band potentials and the electron transfer between CdS and TiO_2 semiconductors. These results showed that the MWCNTs/TiO_2/CdS composite prepared in this study was effective and feasible for use in the decolorization of dye-containing wastewater.

Keywords: TiO_2/CdS; MWCNTs; Photocatalysis; Methyl orange; Operational parameters

1. Introduction

Textile plant effluents have become an issue of worldwide concern due to their strong color that render them visible even at low concentrations, thus causing serious esthetic and pollution problems in wastewater disposal [1,2]. The decolorization and degradation of dyes in textile wastewater continues to be a problematic issue since these azo dyes are relatively resistant to conventional biological treatment methods [3,4]. The pretreatment of dyes in wastewater by photocatalytic processes using TiO_2 has been researched during the last few years to improve the biodegradability of raw dyes in wastewater before the second biological coupling stage [5]. Unfortunately, owing to the large energy band gap of 3.2 eV, normal anatase TiO_2 needs ultraviolet (UV) irradiation to initiate its photoactivity, which greatly hinders the utilization of TiO_2 photocatalysis [1,6,7]. Therefore significant efforts have been made to develop photocatalysts to utilize the visible light which accounts for the largest proportion of the solar spectrum and artificial light sources [8].

Composites of TiO_2 and other semiconducting materials with different band gaps and band positions have been investigated as this produces a long distance charge separated state with electrons and holes at sites far from each other. Of these composites, TiO_2/CdS is an excellent candidate for the photodecomposition of pollutants, as a result of its intrinsic energy band gap [9–12]. However, such particles aggregate easily which diminishes the specific area of the composite and negatively affects the photocatalytic performance. There have been some proposals to solve this problem, such as immobilizing the particles on solid carriers [13]. Considering the unique electrical properties and high chemical stability of multi-walled carbon nanotubes (MWCNTs), it is expected that the combination of MWCNTs with TiO_2/CdS particles may induce charge transfer and immobilize the particles. Furthermore, some authors

*Corresponding author. Tel./fax: +86 750 3299391.
E-mail address: wyuchemxs@126.com (S. Xie).

0272-8842/$ - see front matter © 2013 Elsevier Ltd and Techna Group S.r.l. All rights reserved.
http://dx.doi.org/10.1016/j.ceramint.2013.03.073

have reported that MWCNTs increase the adsorption and photocatalytic activity of TiO_2 [14–16]. The photocatalytic properties of MWCNTs/TiO_2/CdS composite photocatalysts still remain largely unexplored, although a few studies have focused on the preparation of the composite [1,11]. However, these works were mainly focused on the aspects of its materials science [17], while the effects of key reaction conditions, such as catalyst dosage, pH, the coexisting anions commonly contained in wastewater and the addition of H_2O_2, on the photocatalytic reaction when using the MWCNTs/TiO_2/CdS composite have not been well investigated.

The aim of this work was to study the decolorization of methyl orange (MO) by means of MWCNTs/TiO_2/CdS composite photocatalysis; in particular, with regard to the effect of the operating conditions, such as catalyst loading, substrate initial concentration, solution pH and coexisting anions, on decolorization. Moreover, the efficiency of ultrasound in decolorizing the solution, either alone or in conjunction with visible light irradiation, was evaluated. The mechanism of photocatalytic degradation under visible irradiation was also investigated. The aim of the study was to provide fundamental information for the practical treatment of dye wastewater under solar light irradiation.

2. Methods and materials

2.1. Materials

Raw MWCNTs (length 10–30 nm) was obtained from Shenzhen Nanotech Port Co., Shenzhen, China. Titanium (IV) butoxide ($Ti(OBu)_4$, AR) was purchased from Tianjin YongDa Chemical Regent Co. Ltd., Tianjin, China. MO, AR, ($C_{14}H_{14}O_3N_3SNa$, molecular weight = 327.35 g mol^{-1}) were purchased from XiLong Fine Chemical Reagent Co. Ltd., Shantou, China. All other reagents used in this study, including chloroform, nitric acid, hydrochloric acid, cadmium nitrate, sodium hydroxide, anhydrous ethanol and acetic acid, were all AR grade and were obtained from Tianjin DaMao Chemical Reagent Co. Ltd., Tianjin, China. Deionized water was used for the preparation of the photocatalysts. All the reagents were used without any further purification. 0.1 mol/L^{-1} NaOH or 0.1 mol/L^{-1} HCl was used to adjust the pH value of solutions.

2.2. Preparation and characterization of MWCNTs/TiO_2

TiO_2 and MWCNTs/TiO_2/CdS composite photocatalysts were prepared through a sol–gel method modified from Huang et al. [11]. The procedure was as follows: 0.92 g Cd $(NO_3)_2 \cdot 4H_2O$ and 0.73 g $Na_2S \cdot 9H_2O$ were introduced into two beakers each containing 10 mL ethanol. After the solutions were stirred magnetically for 10 min, the sodium sulfide solution was added to the cadmium nitrate solution dropwise under stirring. The mixture was then stirred for 2 h and a light yellow gel formed. Then 0.048 g MWCNTs pretreated with 69% nitric acid was added to a flask containing 10 mL of $Ti(OC_4H_9)_4$, 30 mL of ethanol and 3 mL of anhydrous acetic acid. The mixture was stirred magnetically for 2 h and then the yellow gel, 20 mL of anhydrous ethanol, 2 mL of nitric acid and 4 mL of deionized water were added dropwise. After 6 h of stirring, the resulting colloidal solution was aged for 30 h and then the solvent was evaporated at 80 °C. The solvent was dried at 80 °C for at least 24 h. Finally, the obtained solid was calcined at 500 °C under N_2 for 2 h to obtain a MWCNTs/TiO_2/CdS composite. For comparison, TiO_2 was prepared using similar procedures. The XRD patterns were obtained with an X'Pert PRO advance diffractometer (Panalytical, The Netherlands). The UV–visible absorption was measured by using a UV–vis spectrophotometer (Helios Alpha, UK).

2.3. Photocatalytic activities

To simulate the sunlight spectrum, a 300 W Xe arc lamp (BL-GHX-CH500, Xi'an Depai Biotech. Co. Ltd., Xi'an, China) was applied as the light source; this was positioned inside a cylindrical Pyrex vessel surrounded by a circulating water jacket to cool the lamp. For a typical experiment, 0.12 g of catalyst was put into 100 mL of 20 mg/L methyl orange aqueous solution with stirring in darkness for 30 min to reach the adsorption–desorption equilibrium of MO on the catalyst surface prior to illumination. The suspension was then exposed to light with continuous magnetic stirring [18]. Then 4 mL of suspensions were collected and centrifugally separated every 10 min, and the filtrate was returned to the beaker after the concentration of MO in supernatant was measured using a UV–vis spectrophotometer (Helios Alpha, UK) at 464 nm.

3. Results and discussion

3.1. X-ray diffraction

The X-ray diffraction (XRD) patterns of TiO_2 and MWCNTs/TiO_2/CdS composites are shown in Fig. 1. The diffraction peaks at $2\theta = 25.3$, 37.8, 48.1 and 54.1 were attributed to anatase-TiO_2, and the diffraction peaks at $2\theta = 27.5$, 36.2, 41.4 and 54.4 to

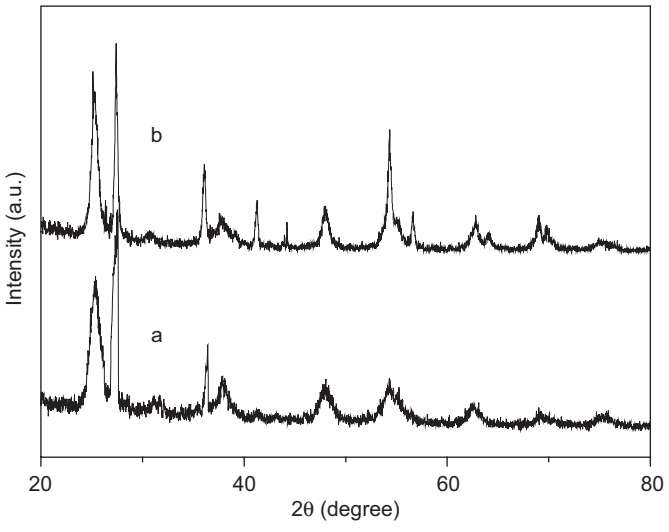

Fig. 1. X-ray diffraction patterns of (a) TiO_2 and (b) MWCNTs/TiO_2/CdS composite.

rutile-TiO_2 [19]. Meanwhile, the diffraction peaks at $2\theta = 26.3$, 28.2, 43.7 and 47.5 were attributed to the hexagonal CdS phase [20], which revealed the successful formation of this phase in the composite. In the samples, the peak for carbon could not be recognized because of its amorphous structure and the small amount present in the composites. The XRD pattern of the TiO_2 contained the same characteristic peaks as that of the MWCNTs/TiO_2/CdS composites (major peaks: 25.3, 27.5, 37.8, 48.1, 54.1 and 54.4). The XRD results confirmed that anatase TiO_2, rutile TiO_2 and hexagonal CdS coexisted in the MWCNTs/TiO_2/CdS composites.

3.2. UV–vis spectra changes of MO with reaction time

To demonstrate changes of molecular and structural characteristics of MO in the presence of MWCNTs/TiO_2/CdS under simulated solar light irradiation, the typical irradiation time dependent UV–vis spectra were measured for a suspension containing 20 mg/L MO at 6.0 pH and 1.2 g/L catalyst loading (Fig. 2). As can clearly be seen, MO exhibited one characteristic absorbance band at 464 nm in the visible region and another absorbance band in the UV region at 273.0 nm, which were attributed to a conjugated structure constructed via the azo bond (–N═N–) and its associated chromophores and auxochromes [21]. The characteristic absorbance band progressively disappeared upon solar irradiation and no new peak appeared during visible light irradiation, indicating that MO was degraded gradually.

3.3. Operational parameters during degradation of MO

3.3.1. Effect of catalyst dosage

Fig. 3 shows the effect of the MWCNTs/TiO_2/CdS composite dosage on the degradation rate of MO using a fixed initial MO concentration (20 mg/L) and for the same irradiation time (90 min). When the concentration of MWCNTs/TiO_2/CdS composite in the suspension was varied from 0.10 to 1.2 g/L, the decolorization rate apparently increased. A further increase to 1.6 g/L in the dosage resulted in a decrease in the degradation rate. The result suggested that at lower levels of catalyst concentrations, increasing the amount of catalyst provided more total surface area and active sites for both adsorption and photocatalysis, resulting in the enhancement of the degradation efficiency. However, any further increase in the catalyst loading over 1.2 g/L might result in the agglomeration of the catalyst, rendering a significant fraction of the catalyst inaccessible to either adsorption of molecules or radiation; this decrease in the active sites available to the catalytic reaction, consequently led to a decrease in the decolorization efficiency. Additionally, it is important to keep the cost of the treatment low if it is to be used industrially. So, the optimum catalyst loading was about 1.2 g/L.

3.3.2. Effect of initial MO concentration

The effect of the initial dye concentration on the photodegradation of MO was also investigated. The initial concentration of MO varied from 10 to 50 mg/L and all solutions were kept at natural pH. The results are shown in Fig. 4. After 80 min of irradiation, the residual MO concentrations were 0.13, 0.45, 4.18, 10.44 and 18.86 mg/L at initial concentrations

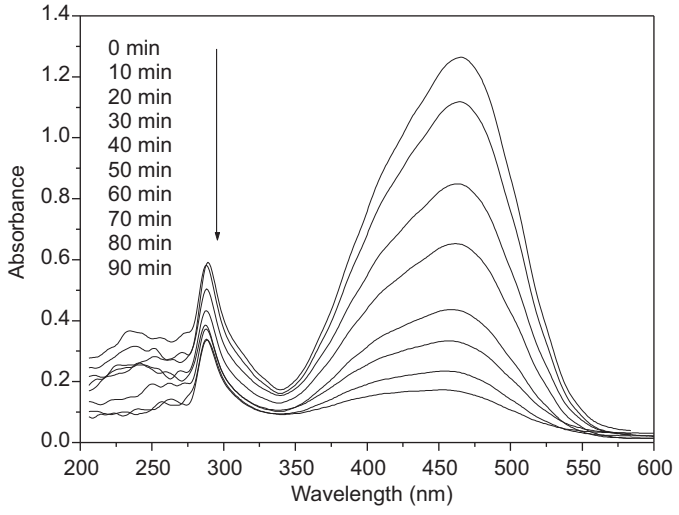

Fig. 2. Ultraviolet–visible spectra of methyl orange solutions with reaction time.

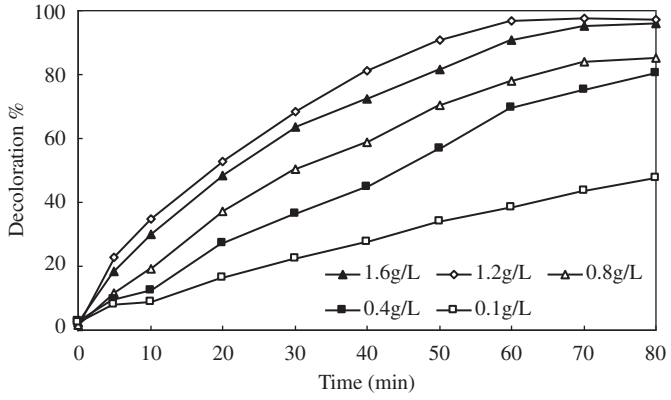

Fig. 3. Effect of composite dosage on the decolorization (concentration of methyl orange = 20 mg/L).

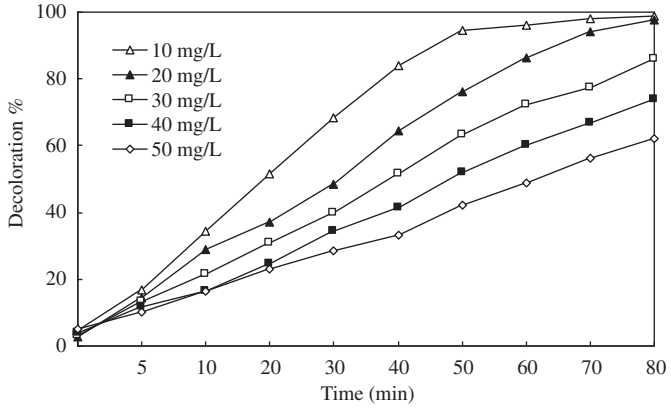

Fig. 4. Effect of initial methyl orange concentration on its decolorization (catalyst amount = 1.2 g/L).

of 10, 20, 30, 40 and 50 mg/L, respectively (Fig. 4). When the other factors were under the same conditions, it can be seen that the efficiency of color removal decreased as the initial dye concentration increased.

A possible explanation for this behavior was that as the initial dye concentration increased, the color of reaction solution became more intense when exposed to the simulated solar light irradiation. Thus the photocatalytic decolorization efficiency decreased since the path length of the photons entering the solution decreased [21]. At the same time, at a higher initial dye concentration, the dye competed with OH^- absorbed on the active sites of MWCNTs/TiO_2/CdS composite surface. Consequently, the number of OH^- on the active sites reduced. As is well known, hydroxyl radicals ($^{\bullet}OH$) are produced by the reaction of photogenerated holes and OH^- ($OH^- + h^+ \rightarrow {}^{\bullet}OH$). The formation of hydroxyl radicals should be the rate-determining step of the photodegradation reaction due to their direct reaction with aromatic compounds. So, as the initial concentration of MO increased, the number of generated $^{\bullet}OH$ radicals decreased. Consequently, the degradation efficiency decreased at higher dye concentrations [22].

3.3.3. Effect of initial pH

It is well known that pH influences the rate of photocatalytic degradation of some organic compounds; the pH of the solution determines the surface charge properties of TiO_2, the charge of the dye molecules and the adsorption of dyes onto the MWCNTs/TiO_2/CdS composite surface [23,24]. Fig. 5 shows MO decolorization as a function of irradiation time at different pH values. As can be seen, decolorization depended strongly on the solution pH: it was substantially reinforced by acidic conditions, while hampered by alkaline conditions. The initial concentration of MO was 20 mg/L and the amount of catalyst was 1.2 g/L. After 30 min of irradiation, the decolorization efficiencies of MO were 80.8%, 55.1%, 47.4%, 42.1% and 35.3% at pH values of 2.6, 4.4, 6.4, 9.4 and 11.1, respectively. After 70 min of irradiation, the corresponding decolorization efficiency was 98.6%, 96.3%, 92.5%, 89.5% and 71.0%, respectively.

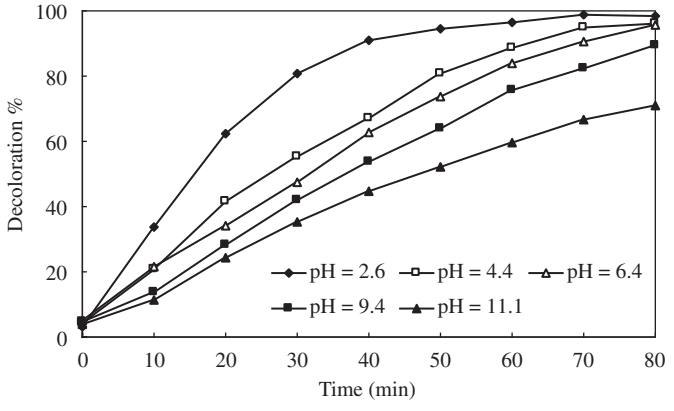

Fig. 5. Effect of initial pH on decolorization (concentration of methyl orange = 20 mg/L, amount of catalyst = 1.2 mg/L).

These findings could be explained in terms of the amphoteric behavior of TiO_2. The solution pH influenced the ionization state of the TiO_2 surface according to the following reactions:

$$Ti\text{–}OH + H^+ = Ti\text{–}OH_2^+ \quad (1)$$

$$Ti\text{–}OH + OH^- = Ti\text{–}O^- + H_2O \quad (2)$$

The charges on TiO_2 surface was different on the basis of the zero-point charge (zpc) of TiO_2; the zpc value for TiO_2 was about 6.5 according to a number of previous reports [2,22–25]. At pH < 6.5, the surface of TiO_2 was positively charged and absorbed negatively charged MO molecules by electrostatic attraction, while at pH > 6.5 it became negatively charged and the absorption of MO molecules became weaker due to repulsive forces. Thus, the electrostatic attraction between the positive charged surface and the negative dye would result in increased degradation under acidic conditions.

3.3.4. Effect of coexisting anions

The existence of inorganic anions such as chloride (Cl^-), nitrate (NO_3^-), carbonate (CO_3^{2-}), sulfate (SO_4^{2-}) and phosphate (PO_4^{3-}) is very common in wastewater [17,21]. Therefore the effect of anions on the photoreaction of organic pollutants should not be neglected. Fig. 6 shows the effects of different anions at the same concentration of 0.01 M solution of their corresponding sodium salts for 20 mg/L initial MO concentration with 1.2 g/L of MWCNTs/TiO_2/CdS composite. The pH of the solution was adjusted to 4.0. The results indicated that the presence of all anions had an inhibitory effect on the decolorization of MO. The order of inhibitory extent was as follows: no anion addition < nitrate < chloride < sulfate < carbonate < phosphate. The strongest inhibition of MO degradation resulted from PO_4^{3-}.

As is well known, the photocatalytic process mainly occurs on the photocatalyst surface, rather than in the bulk solution. So, the adsorption of MO on the active site of TiO_2 surface was very important for the photocatalytic reaction rate. As mentioned for Fig. 5, at pH < 6.5, the TiO_2 surface was positively charged. So the anions such as chloride (Cl^-), nitrate (NO_3^-),

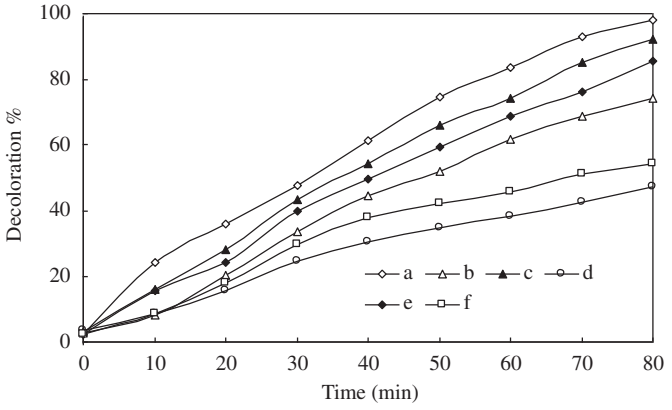

Fig. 6. Effect of coexisting anions on the decolorization (concentration of methyl orange = 20 mg/L, amount of catalyst = 1.2 mg/L): (a) no anions; (b) SO_4^{2-}; (c) NO_3^-; (d) PO_4^{3-}; (e) Cl^-; (f) CO_3^{2-}.

carbonate (CO_3^{2-}), sulfate (SO_4^{2-}) and phosphate (PO_4^{3-}) could be adsorbed onto the positively charged surface of the catalyst by electrostatic attraction, leading to competitive adsorption [17]. Actually, the higher the valence was, the stronger the competitive adsorption was, which was the reason why PO_4^{3-} was the anion that most strongly inhibited MO adsorption and degradation of all the anions mentioned above. What is more, the anions could react with the positive holes and/or hydroxyl radical, leading to the generation of less reactive radicals than $^{\bullet}OH$, which also had an inhibitory effect on the photodegradation of MO in aqueous solution [3].

3.3.5. Effect of H_2O_2 concentration

The effect of H_2O_2 concentration on MO decolorization was analyzed in the range of 0–30 mmol/L with an initial MO concentration of 40 mg/L, 1.2 g/L of catalyst and an initial pH of 6.0. Fig. 7 shows the decolorization curves of MO on the TiO_2, MWCNTs/TiO_2/CdS composites and H_2O_2-assisted MWCNTs/TiO_2/CdS composite particles. Because of the large band gap energy (3.2 eV for anatase), TiO_2 photocatalysis proceeded only at wavelengths shorter than approximately 400 nm. So TiO_2 had a low photocatalytic activity under visible light, and the decolorization rate was only 41.3% after 80 min of simulated solar light irradiation. For the MWCNTs/TiO_2/CdS composite, the decolorization rate reached the much higher value of 70.4% in 80 min. However, it was not effective enough for practical wastewater treatment under visible light irradiation within a reasonable time. In further experiments, the effects of H_2O_2 addition in the solution at concentrations of 4, 10 and 30 mmol/L were studied. In the sample with and 4 mmol/L H_2O_2 added, the decolorization rates of MO reached about 94.4% within 80 min, which was much higher than that of the MWCNTs/TiO_2/CdS composite without H_2O_2. The sample treated with the addition of 10 mmol/L H_2O_2 exhibited the highest photocatalytic activity; the decolorization rate of MO reached about 98.3% within 80 min. This is attributable to the H_2O_2 facilitating the generation of hydroxyl radicals, which are powerful oxidizing agents to degrade MO and effectively promote the photodecolorization. Interestingly, a further increase in H_2O_2 concentrations to 30 mmol/L impeded the decolorization of MO. As can be seen in Fig. 8, the addition of 30 mmol/L H_2O_2, resulted in a decolorization rate of only 72.4% after 80 min irradiation, which was similar to the photocatalytic run without H_2O_2. This may be explained as follows.

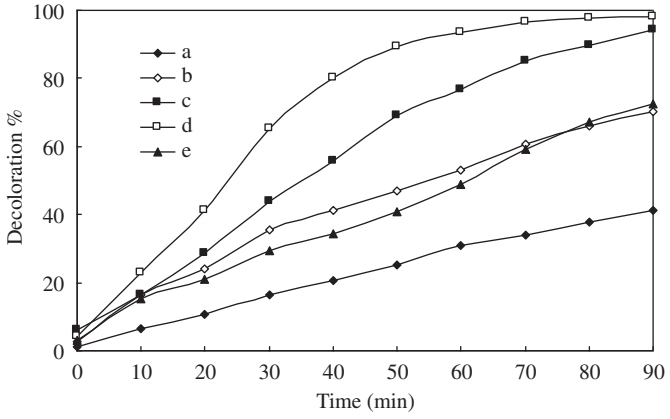

Fig. 7. Effect of addition of H_2O_2 on the decolorization: (a) TiO_2; (b) MWCNTs/TiO_2/CdS; (c) MWCNTs/TiO_2/CdS+4 mm H_2O_2; (d) MWCNTs/TiO_2/CdS+10 mm H_2O_2; (e) MWCNTs/TiO_2/CdS+30 mm H_2O_2 (concentration of methyl orange = 40 mg/L, amount of catalyst = 1.2 g/L).

Hydrogen peroxide plays a dual role in photocatalytic reactions acting as an electron acceptor and also being able to decompose to produce hydroxyl radicals ($OH^{\bullet}$) [26].

$$H_2O_2 + hv \rightarrow 2^{\bullet}OH \quad (3)$$

In addition, it can also inhibit the recombination of electron/hole (e^-/h^+) pairs according to the following equation [27]:

$$H_2O_2 + e^- \rightarrow OH^- + OH^{\bullet} \quad (4)$$

Through the reactions in Eqs. (3) and (4), hydrogen peroxide greatly promoted the photoreaction. However, hydrogen peroxide can also (i) be directly oxidized by the valence band holes (h_{vb}^+) and (ii) react with hydroxyl radicals [2]

$$H_2O_2 + 2h_{vb}^+ \rightarrow O_2 + 2H^+ \quad (5)$$

$$H_2O_2 + {}^{\bullet}OH \rightarrow H_2O + HO_2^- \quad (6)$$

$$H_2O_2 + {}^{\bullet}OH \rightarrow H_2O + O_2 \quad (7)$$

In the above case, the excessive addition of H_2O_2 inhibited the photodecolorization efficiency of MO by scavenging the photogenerated oxidizing species (i.e. valence band holes and hydroxyl radicals) (Eqs. (5)–(7)) [28], which would otherwise be available for the oxidative destruction of the dye molecule.

3.4. Recycling MWCNTs/TiO_2/CdS composite

The photocatalytic stability of the photocatalyst was also studied with the MO (20 mg/L) mixed with 1.2 g/L catalyst under simulated solar irradiation for 90 min. After the photocatalyst was used once, the photocatalyst was dried at 60 °C for 1 h, and then the recovered photocatalyst was reused in the next cycle with the same initial conditions.

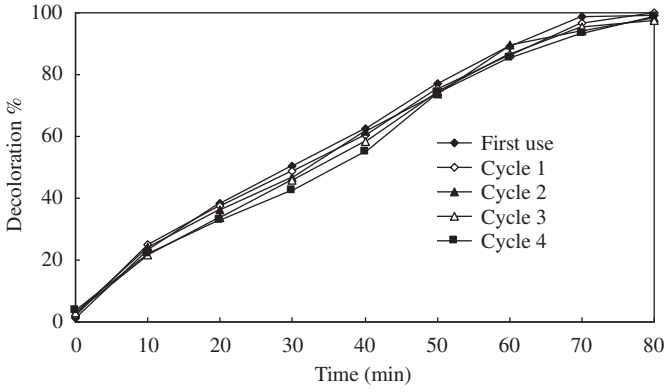

Fig. 8. Reuse of photocatalyst (concentration of methyl orange = 0 mg/L, amount of catalyst = 1.2 g/L).

As shown in Fig. 8, there was no significant reduction in photoactivity observed when the photocatalyst was used five times. The catalytic efficiency of the MWCNTs/TiO_2/CdS composite photocatalyst was still higher than 98.7% at five cycles after 80 min of irradiation, indicating that MWCNTs/TiO_2/CdS composite possessed excellent photocatalytic stability.

3.5. Proposed mechanism of MO degradation

As previously stated, the band gap of anatase TiO_2 was 3.2 eV, pure TiO_2 showed a clear absorption edge below 400 nm, as reported in many papers, and no absorption in the visible light region above 400 nm was observed [29,30,31].

After modification of TiO_2 with CdS supported on MWCNTs, the extension of the optical absorption spectrum into the visible region was expected, because of the suitable band gap of CdS (2.3 eV), which is much lower than that of pure TiO_2. When visible light was supplied to the coupling composite, the electrons on the valence band of CdS were excited and then transferred to the conduction band of TiO_2, then transferred to the composite surface, leaving behind holes in its valence band. This fast electron transfer between two semiconductors may lead to higher quantum efficiency, supplying more generated electrons to be used in photocatalytic reactions. Furthermore, the different band gap structures of two semiconductors promoted the separation efficiency of the electron–hole pairs. So the MWCNTs/TiO_2/CdS composites could be excited to produce more electron–hole pairs under visible light illumination, which could result in the higher photocatalytic activity of the composite under visible light.

The photogenerated electrons were so active that they could react with electron acceptors such as O_2 adsorbed on the surface of TiO_2 or dissolved in water, then yield $^{\bullet}O_2^-$ [32]. At the same time, a positively charged hole (h^+) could react with OH^- or H_2O to generate $^{\bullet}OH$. $^{\bullet}O_2^-$ and $^{\bullet}OH$ are super strong oxidants and were dominant species in the photocatalytic process. These oxidants then oxidized a variety of organic pollutants under light irradiation. Furthermore, the large specific surface area of MWCNTs avoided the aggregation of nanoparticles, diminished the rate of electron–hole recombination and supplied active sites for reaction, which was also favorable for photocatalytic reaction [1,11]. The reactions could be expressed as follows:

$$\text{MWCNTs–CdS–TiO}_2+h\nu \rightarrow \text{MWCNTs–CdS } (h^+,e^-)\text{–TiO}_2 \quad (8)$$

$$\text{MWCNTs–CdS } (h^+,e^-)\text{–TiO}_2 \rightarrow \text{MWCNTs–CdS } (h^+)\text{–TiO}_2\ (e^-) \quad (9)$$

$$O_2+e^- \rightarrow {}^{\bullet}O_2^- \quad (10)$$

$$H_2O+{}^{\bullet}O_2^- \rightarrow {}^{\bullet}HO_2+OH^- \quad (11)$$

$$O_2+H^++{}^{\bullet}HO_2 \rightarrow H_2O_2+O_2 \quad (12)$$

$$OH^-+h^+ \rightarrow {}^{\bullet}OH \quad (13)$$

$$H_2O_2 \rightarrow 2{}^{\bullet}OH \quad (14)$$

$$^{\bullet}O_2^-+MO \rightarrow CO_2+H_2O \quad (15)$$

$$^{\bullet}OH+MO \rightarrow CO_2+H_2O \quad (16)$$

3.6. Coupling photocatalysis with ultrasound

In a final set of experiments, solutions containing 30 mg/L and 60 mg/L MO were subjected to simultaneous simulated solar light and ultrasound irradiation in the presence of 1.2 g/L MWCNTs/TiO_2/CdS composite. These sonophotocatalytic experiments were performed in an apparatus identical to that used for photocatalytic experiments. Magnetic stirring were used to produce a homogeneous suspension of the catalyst in the solution. A KH2200DB Controllable Serial-Ultrasonics apparatus (Kunshan Hechuang Ultrasonic Instrument Co., Ltd, China), operating at ultrasonic frequency of 40 kHz and output power of 80 W, was adopted to irradiate the MO solution.

As can be clearly seen in Fig. 9, no matter whether in 30 or in 60 mg/L MO solution, the decomposition of MO using the sonophotocatalytic system was much faster than when using the photocatalytic system, especially for the higher initial concentration solution. Under simulated solar light alone, after 90 min of irradiation, in 30 mg/L MO solution, the decolorization efficiency of MO was 85.2%, compared to 92.8% for the sonophotocatalytic system; in 60 mg/L MO solution, the corresponding decolorization efficiencies of MO were 58.2% and 79.3%.

The beneficial effect of coupling photocatalysis with sonolysis could be attributed to several reasons [2,33]: (i) ultrasound provided an extra source of hydroxyl radicals from the sonolytic cleavage of water; (ii) acoustic cavitation was able to enhance mass transfer between the liquid phase and the catalyst surface; (iii) acoustic cavitation increased the uniformity of the dispersion, increased catalytic activity due to ultrasound de-aggregating catalyst particles, thus increasing the available surface area; (iv) acoustic cavitation could clean the catalyst surface due to acoustic micro-streaming, which was then available for regenerating more active catalyst sites for reaction. Although the relative contributions of the above effects are difficult to differentiate, the overall net effect was an enhancement in the rate of reaction.

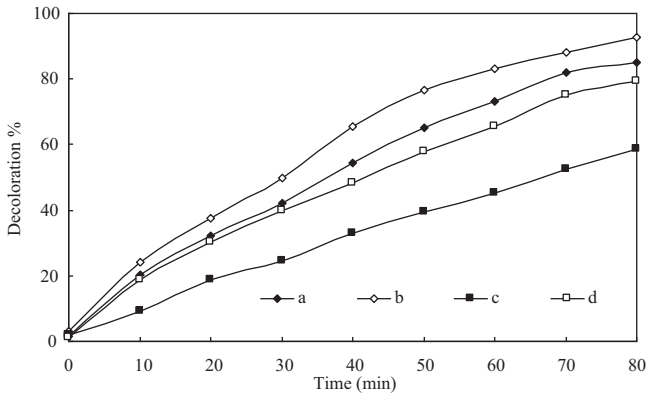

Fig. 9. Decolorization of methyl orange (MO) during combined sonochemical and photocatalytic (sonophotocatalytic) degradation: (a) 30 mg/L MO, photocatalytic decolorization; (b) 30 mg/L MO, sonophotocatalytic decolorization; (c) 60 mg/L MO, photocatalytic decolorization; (d) 60 mg/L MO, sonophotocatalytic decolorization.

4. Conclusion

Composites of TiO_2/CdS nanoparticles supported on MWCNTs with a high activity for MO degradation under simulated solar irradiation could be readily obtained by the sol–gel method. The modified catalysts possessed a strong absorption band in the visible range and showed a higher photocatalytic activity than the neat TiO_2 nanoparticles. The photocatalytic activity of MWCNTs/TiO_2/CdS was examined by degrading MO under simulated solar irradiation; the various operational factors (catalyst dosage, initial MO concentration, solution pH, the addition of H_2O_2 and the coexisting anions) were investigated in detail. A pH value of 2.6, a catalyst dosage of 1.2 g/L with the concentration of 10 mmol/L H_2O_2, as well as a small initial dye concentration (10 mg/L) yielded the optimum photocatalytic degradation performance. All chosen anions had an inhibitory effect on the decolorization of MO and the strongest inhibition resulted from PO_4^{3-}. The photocatalyst showed a good reproducibility and considerable stability. Furthermore, a possible visible light-induced photocatalytic mechanism has been proposed. Coupling photocatalysis with ultrasound irradiation resulted in increased efficiency compared to the individual photodegradation. Overall, it was found that the MWCNTs/TiO_2/CdS composite could be used to efficiently decolorize practical dye wastewater under visible light.

Acknowledgments

This work was financially supported by the Outstanding youth innovative talent cultivation project of Guangdong Province (No. LYM0129) and the Natural Science Foundation of Guangdong Province (No. S2011040000633).

References

[1] H. Wang, H.L. Wang, W.F. Jiang, Solar photocatalytic degradation of 2,6-dinitro-p-cresol (DNPC) using multi-walled carbon nanotubes (MWCNTs)–TiO_2 composite photocatalysts, Chemosphere 75 (2009) 1105–1111.

[2] D.E. Kritikos, N.P. Xekoukoulotakis, E. Psillakis, D. Mantzavinos, Photocatalytic degradation of reactive black 5 in aqueous solutions: Effect of operating conditions and coupling with ultrasound irradiation, Water Research 41 (2007) 2236–2246.

[3] H.Y. Zhu, L. Xiao, R. Jiang, G.M. Zeng, L. Liu, Efficient decolorization of azo dye solution by visible light-induced photocatalytic process using SnO_2/ZnO heterojunction immobilized in chitosan matrix, Chemical Engineering Journal 172 (2011) 746–753.

[4] C.S. Pan, Y.F. Zhu, New type of $BiPO_4$ oxy-acid salt photocatalyst with high photocatalytic activity on degradation of dye,, Environmental Science and Technology 44 (2010) 5570–5574.

[5] M. Shang, W.Z. Wang, S.M. Sun, J. Ren, L. Zhou, L. Zhang, Efficient visible light induce photocatalytic degradation of contaminant by spindle-like PANI/$BiVO_4$, Journal of Physical Chemistry C 113 (2009) 20228–20233.

[6] R. Wang, D. Xu, J.B. Liu, K.W. Li, H. Wang, Preparation and photocatalytic properties of CdS/$La_2Ti_2O_7$ nanocomposites under visible light, Chemical Engineering Journal 168 (2011) 455–460.

[7] B. Zhang, J.K. Jian, Y. Zheng, Y. Sun, Y. Chen, L. Cui, Low temperature hydrothermal synthesis of CdS submicro- and microspheres self-assembled from nanoparticles, Materials Letters 62 (2008) 1827–1830.

[8] Z. Liu, Z.G. Zhao, M. Miyauchi, Efficient visible light active $CaFe_2O_4$/WO_3 based composite photocatalysts: effect of interfacial modification, Journal of Physical Chemistry C 113 (2009) 17132–17137.

[9] W.W. So, K.J. Kim, S.J. Moon, Photo-production of hydrogen over the CdS-TiO_2 nano-composite particulate films treated with $TiCl_4$, International Journal of Hydrogen Energy 29 (2004) 229–234.

[10] H. Park, W. Choi, M.R. Hoffmann, Effects of the preparation method of the ternary CdS/TiO_2/Pt hybrid photocatalysts on visible light-induced hydrogen production, Journal of Materials Chemistry 18 (2008) 2379–2385.

[11] B.C. Huang, Y. Yang, X.S. Chen, D.Q. Ye, Preparation and characterization of CdS–TiO_2 nanoparticles supported on multi-walled carbon nanotubes, Catalysis Communications 11 (2010) 844–847.

[12] J.S. Jang, H.G. Kim, P.H. Borse, J.S. Lee, Simultaneous hydrogen production and decomposition of H_2S dissolved in alkaline water over CdS–TiO_2 composite photocatalysts under visible light irradiation, International Journal of Hydrogen Energy 32 (2007) 4786–4791.

[13] Q. Wang, D. Yang, D.M. Chen, Y.B. Wang, Z.Y. Jiang, Synthesis of anatase titania–carbon nanotubes nanocomposites with enhanced photocatalytic activity through a nanocoating–hydrothermal process, Journal of Nanoparticle Research 9 (2007) 1087–1096.

[14] C.Y. Kuo, Prevenient dye-degradation mechanisms using UV/TiO_2/carbon nanotubes process, Journal of Hazardous Materials 163 (2009) 239–244.

[15] H.T. Yu, X. Quan, S. Chen, H.M. Zhao, Y.B. Zhang, TiO_2–carbon nanotube heterojunction arrays with a controllable thickness of TiO_2 layer and their first application in photocatalysis, Journal of Photochemistry and Photobiology A: Chemistry 200 (2008) 301–306.

[16] B. Gao, C. Peng, G.Z. Chen, G.L. Puma, Photo-electro-catalysis enhancement on carbon nanotubes/titanium dioxide (CNTs/TiO_2) composite prepared by a novel surfactant wrapping sol–gel method, Applied Catalysis B: Environmental 85 (2008) 17–23.

[17] H.C. Liang, X.Z. Li, Y.H. Yang, K.H. Sze, Effects of dissolved oxygen, pH, and anions on the 2,3-dichlorophenol degradation by photocatalytic reaction with anodic TiO_2 nanotube films, Chemosphere 73 (2008) 805–812.

[18] J. Fang, F.C. Shi, J. Bu, J.J. Ding, S.T. Xu, J. Bao, Y.S. Ma, Z.Q. Jiang, W.P. Zhang, C. Gao, W.X. Huang, One-step synthesis of bifunctional TiO_2 catalysts and their photocatalytic activity, Journal of Physical Chemistry C 114 (2010) 7940–7948.

[19] W.X. Zhao, Z.P. Bai, A.L. Ren, B. Guo, C. Wu, Sunlight photocatalytic activity of CdS modified TiO_2 loaded on activated carbon fibers, Applied Surface Science 256 (2010) 3493–3498.

[20] Y. Kang, D. Kim, Enhanced optical sensing by carbon nanotube functionalized with CdS particles, Sensors and Actuators A: Physical 125 (2006) 114–117.

[21] H.Y. Zhu, R. Jiang, Y.J. Guan, Y.Q. Fu, L. Xiao, G.M. Zeng, Effect of key operational factors on decolorization of methyl orange during H_2O_2 assisted CdS/TiO_2/polymer nanocomposite thin films under simulated solar light radiation, Separation and Purification Technology 74 (2010) 187–194.

[22] H.L. Li, L.X. Cao, W. Liu, G. Su, B.H. Dong, Synthesis and investigation of TiO_2 nanotube arrays prepared by anodization and their photocatalytic activity, Ceramics International 38 (2012) 5791–5797.

[23] K.E. O'Shea, E. Pernas, J. Saiers, The influence of mineralization products on the coagulation of TiO_2 photocatalyst, Langmuir 15 (1999) 2071–2076.

[24] A.G. Rincón, C. Pulgarin, Effect of pH, inorganic ions matter and H_2O_2 on *E. coli* K12 photocatalytic inactivation by TiO_2 implications in solar water disinfection, Applied Catalysis B: Environmental 51 (2004) 281–300.

[25] J. Grzechulska, A.W. Morawski, Photocatalytic decomposition of azo-dye acid black 1 in water over modified titanium dioxide, Applied Catalysis B: Environmental 36 (2002) 45–51.

[26] C.G. Silva, J.L. Faria, Effect of key operational parameters on the photocatalytic oxidation of phenol by nanocrystalline sol–gel TiO_2 under UV irradiation, Journal of Molecular Catalysis A—Chemical 305 (2009) 147–154.

[27] Z.C. Guo, B. Chen, J.B. Mu, M.Y. Zhang, P. Zhang, Z.Y. Zhang, J. F. Wang, X. Zhang, Y.Y. Sun, C.L. Shao, Y.C. Liu, Iron phthalocyanine/TiO_2 nanofiber heterostructures with enhanced visible photocatalytic activity assisted with H_2O_2, Journal of Hazardous Materials 219–220 (2012) 156–163.

[28] Z.H. Wang, W.H. Ma, C.C. Chen, J.C. Zhao, Light-assisted decomposition of dyes over iron-bearing soil clays in the presence of H_2O_2, Journal of Hazardous Materials 168 (2009) 1246–1252.

[29] Y.J. Li, X.D. Li, J.W. Li, J. Yin, Photocatalytic degradation of methyl orange by TiO_2-coated activated carbon and kinetic study, Water Research 40 (2006) 1119–1126.

[30] X. Zhang, L. Lei, J. Zhang, Q. Chen, J. Bao, B. Fang, A novel CdS/S–TiO_2 nanotubes photocatalyst with high visible light activity, Separation and Purification Technology 66 (2009) 417–421.

[31] R. Asahi, T. Morikawa, T. Ohwaki, K. Aoki, Y. Taga, Visible-light photocatalysis in nitrogen-doped titanium oxides, Science 293 (2001) 269–271.

[32] S. Shanmugasundaram, K. Horst, Daylight photocatalysis by carbon-modified titanium dioxide, Angewandte Chemie International Edition 42 (2003) 4908–4911.

[33] N. Shimizu, C. Ogino, M.F. Dadjour, T. Murata, Sonocatalytic degradation of methylene blue with TiO_2 pellets in water, Ultrasonics Sonochemistry 14 (2007) 184–190.